7-2010

Porosity detection in ceramic armor tiles via ultrasonic time-of-flight

Frank J. Margetan
Iowa State University, fmargeta@iastate.edu

Nathaniel L. Richter
Iowa State University

Terrence C. Jensen
Iowa State University, tcjensen@iastate.edu

Porosity detection in ceramic armor tiles via ultrasonic time-of-flight

Abstract
Some multilayer armor panels contain ceramic tiles as one constituent, and porosity in the tiles can affect armor performance. It is well known that porosity in ceramic materials leads to a decrease in ultrasonic velocity. We report on a feasibility study exploring the use of ultrasonic time-of-flight (TOF) to locate and characterize porous regions in armor tiles. The tiles in question typically have well-controlled thickness, thus simplifying the translation of TOF data into velocity data. By combining UT velocity measurements and X-ray absorption measurements on selected specimens, one can construct a calibration curve relating velocity to porosity. That relationship can then be used to translate typical ultrasonic C-scans of TOF-versus-position into C-scans of porosity-versus-position. This procedure is demonstrated for pulse/echo, focused-transducer inspections of silicon carbide (SiC) ceramic tiles.

Keywords
X-ray absorption, multilayers, porous materials, ceramics, nondestructive evaluation, QNDE, Aerospace Engineering

Disciplines
Aerospace Engineering | Materials Science and Engineering | Structures and Materials

This article appeared in *AIP Conference Proceedings* 1335 (2011): 1037–1044 and may be found at http://dx.doi.org/10.1063/1.3592051.

POROSITY DETECTION IN CERAMIC ARMOR TILES VIA ULTRASONIC TIMEOFFLIGHT

Frank J. Margetan, Nathaniel Richter, and Terrence Jensen

Citation: AIP Conf. Proc. **1335**, 1037 (2011); doi: 10.1063/1.3592051
View online: http://dx.doi.org/10.1063/1.3592051
View Table of Contents: http://proceedings.aip.org/dbt/dbt.jsp?KEY=APCPCS&Volume=1335&Issue=1
Published by the American Institute of Physics.

POROSITY DETECTION IN CERAMIC ARMOR TILES VIA ULTRASONIC TIME-OF-FLIGHT

Frank J. Margetan, Nathaniel Richter, and Terrence Jensen

Center for Nondestructive Evaluation, Iowa State University, Ames, IA 50011

ABSTRACT. Some multilayer armor panels contain ceramic tiles as one constituent, and porosity in the tiles can affect armor performance. It is well known that porosity in ceramic materials leads to a decrease in ultrasonic velocity. We report on a feasibility study exploring the use of ultrasonic time-of-flight (TOF) to locate and characterize porous regions in armor tiles. The tiles in question typically have well-controlled thickness, thus simplifying the translation of TOF data into velocity data. By combining UT velocity measurements and X-ray absorption measurements on selected specimens, one can construct a calibration curve relating velocity to porosity. That relationship can then be used to translate typical ultrasonic C-scans of TOF-versus-position into C-scans of porosity-versus-position. This procedure is demonstrated for pulse/echo, focused-transducer inspections of silicon carbide (SiC) ceramic tiles.

Keywords: Ceramic Armor, Silicon Carbide, Porosity, Ultrasonic Velocity, Ultrasonic Time-of-Flight
PACS: 43.20.Jr, 43.20.Ye.

INTRODUCTION

Ceramic materials have a wide variety of uses, including as energy-absorbing layers in advanced armors. Porosity caused by insufficient compaction during manufacture can degrade the strength of ceramics leading to armor failure. In this paper we investigate the feasibility of using ultrasonic pulse/echo Time-of-Flight (TOF) to determine porosity levels in silicon-carbide (SiC) ceramic tiles. Most UT scanning systems have built-in options for acquiring and displaying C-scan images of ultrasonic TOF versus position. It is well known that for ceramic materials an increase in porosity leads to a decrease in sound velocity [1]. Here, using a small group of ceramic specimens with different porosity levels, we perform standard, normal incidence, pulse/echo ultrasonic C-scans of back-wall amplitude and TOF. We then use UT and X-ray measurements to establish the relationship between sound speed variations and density variations. That relationship is then used to translate the ultrasonic TOF C-scan images into porosity images.

TILE SPECIMENS AND TIME-OF-FLIGHT MEASUREMENTS

Hexagonal silicon carbide tiles, some fully compacted and some having porous regions, were supplied to us by BAE Systems. The tiles measured 0.75" thick by 4.0" across (edge-to-edge), and were of the same type used in a prototype 5-layer armor design studied last year [2]. Three of the tiles spanning a range of porosity were selected for detailed examination in our

Review of Progress in Quantitative Nondestructive Evaluation, Volume 30
AIP Conf. Proc. 1335, 1037-1044 (2011); doi: 10.1063/1.3592051

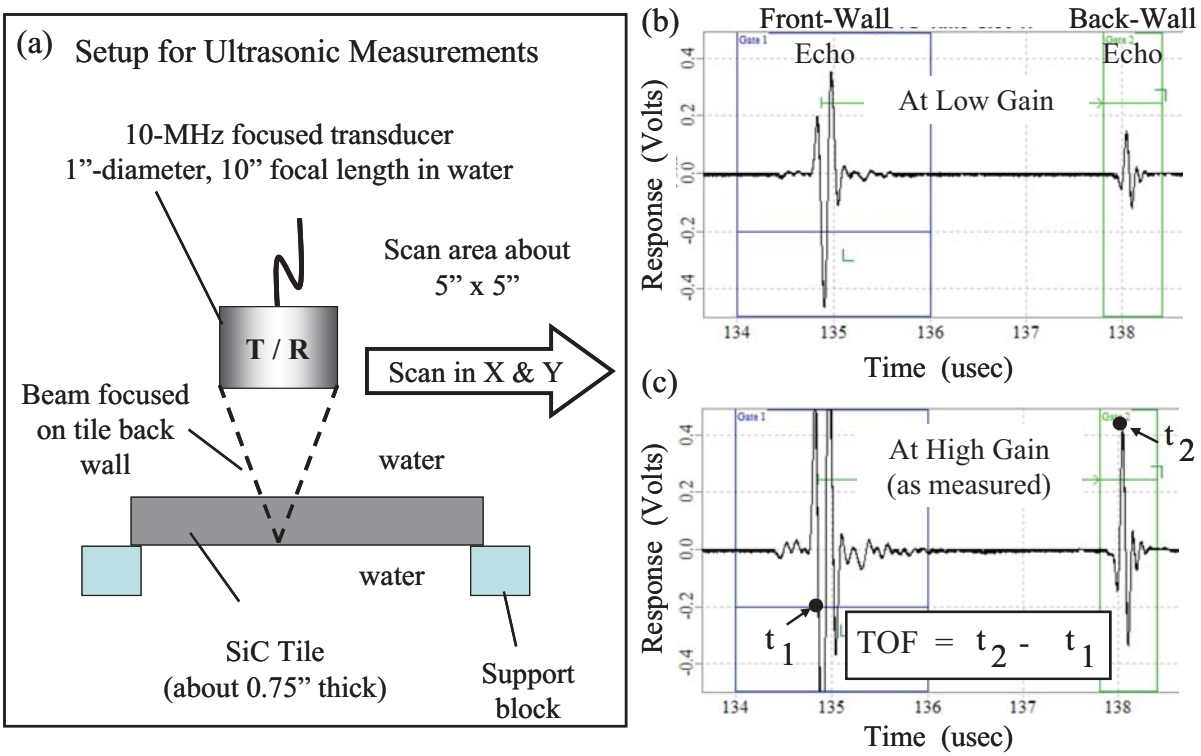

FIGURE 1. (a) Equipment setup for ultrasonic C-scans of tiles. (b)-(c) Examples of front-wall and back-wall echoes from a tile at both low inspection gain and the higher gain used for measurements.

feasibility study. As illustrated in Figure 1, a normal-incidence, ultrasonic, pulse/echo immersion scan was performed on each specimen using a 10-MHz spherically-focused transducer. The inspection water path was set to about 3.92 inches so that the measured focus was located near the specimen back wall. The transducer was scanned in the two lateral dimensions above the specimen using a step size of 0.05 inches. A standard "front-surface following" time gate was used to acquire and store RF waveforms. By using this common feature of ultrasonic scanning systems, the stored waveforms are relatively insensitive to minor misalignments in which the scanning axes are not parallel to the upper surface of the specimen. As illustrated in Figure 1c, the inspection gain was set such that the front-wall response was saturated and the back-wall response filled most of the available screen height. We used a UTEX data acquisition system having an 8-bit digitizer and sampling rate of 500 MHz.

Time-of-flight C-scan images were constructed in which the displayed time was the interval between: (1) the moment the (saturated) front-wall echo first crossed a preset negative voltage threshold level; and (2) the time of the dominant positive peak in the back-wall echo. (See t_1 and t_2 in Figure 1c.) Amplitude C-scan images, displaying the peak positive voltage of the back-wall echo were also constructed from the stored data. For the three ceramic tiles in question, the TOF and amplitude C-scans are shown in Figure 2. Variations in TOF were clearly evident, with measured TOF values ranging from about 100% to 106% of that of the unflawed tile. Variations in back-wall amplitude were also seen, with measured amplitudes ranging from about 92% to 100% of that of the unflawed tile. Presumably, either TOF or amplitude could be used as a basis for estimating porosity levels. However, amplitude variations, unlike TOF variations, are expected to be strongly frequency dependent and thus require more careful analysis. Thus, here we concentrate on using the TOF data alone.

At a given transducer position, the relationship between the measured TOF and the average sound velocity in the tile is expected to have the form

$$velocity = 2(tile\ thickness)/(TOF - t_{shift}) \quad . \qquad (1)$$

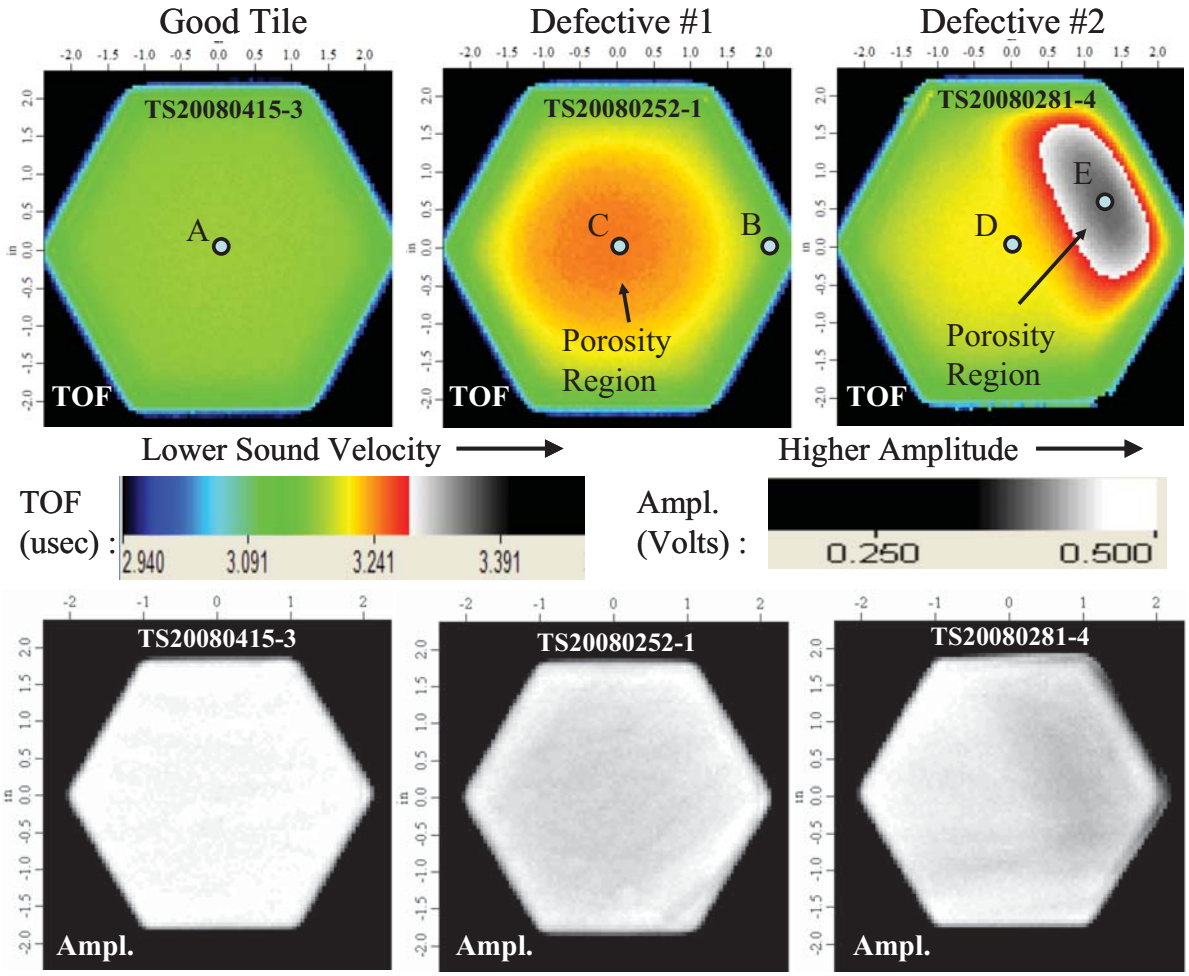

FIGURE 2. C-scan images of time–of-flight (upper row) and amplitude (lower row) for ultrasonic inspections of three hexagonal SiC tiles. The gray scale for the amplitude images has high contrast at the higher amplitudes. Thus low amplitudes near tile edges are rendered black, reducing the apparent size.

Consulting Figure 1, a phase reversal is expected between the front and back wall echoes of the tile. Thus, the time shift t_{shift} may be thought of as accounting for the difference between the time t_1 when the voltage threshold is crossed and the time of the negative peak in the front-wall signal. In addition, the shift accounts for the subtle effect of focusing on the phases of the two signals. Note that t_{shift} is dependent on the measurement setup since the choices of inspection water path, gain setting and threshold level all effect t_{shift}. Before time-of-flight values can be mapped into velocity values, t_{shift} must be determined for the specific measurement setup being used, and the tile thickness must be known. Fortunately, in armor applications, the thickness of the tiles is usually fixed within a tight tolerance, so thickness variation per se has little impact on time-of-flight. For the three tiles shown in Figure 2, thickness differences were no more than 0.001 inch or 0.13 %.

ULTRASONIC VELOCITY MEASUREMENTS

We next made accurate sound velocity measurements at five locations on the tiles having different TOF values, and hence presumably different porosity levels. These locations are marked A, B, C, D and E on Figure 2. The speeds of both longitudinal and shear wave were measured, although we are primarily interested only in the former. As shown in Figure 3a, 0.25-inch diameter planar transducers were used, having center frequencies of 25 MHz for the longitudinal wave mode (water immersion measurement) and 5 MHz for the shear wave mode

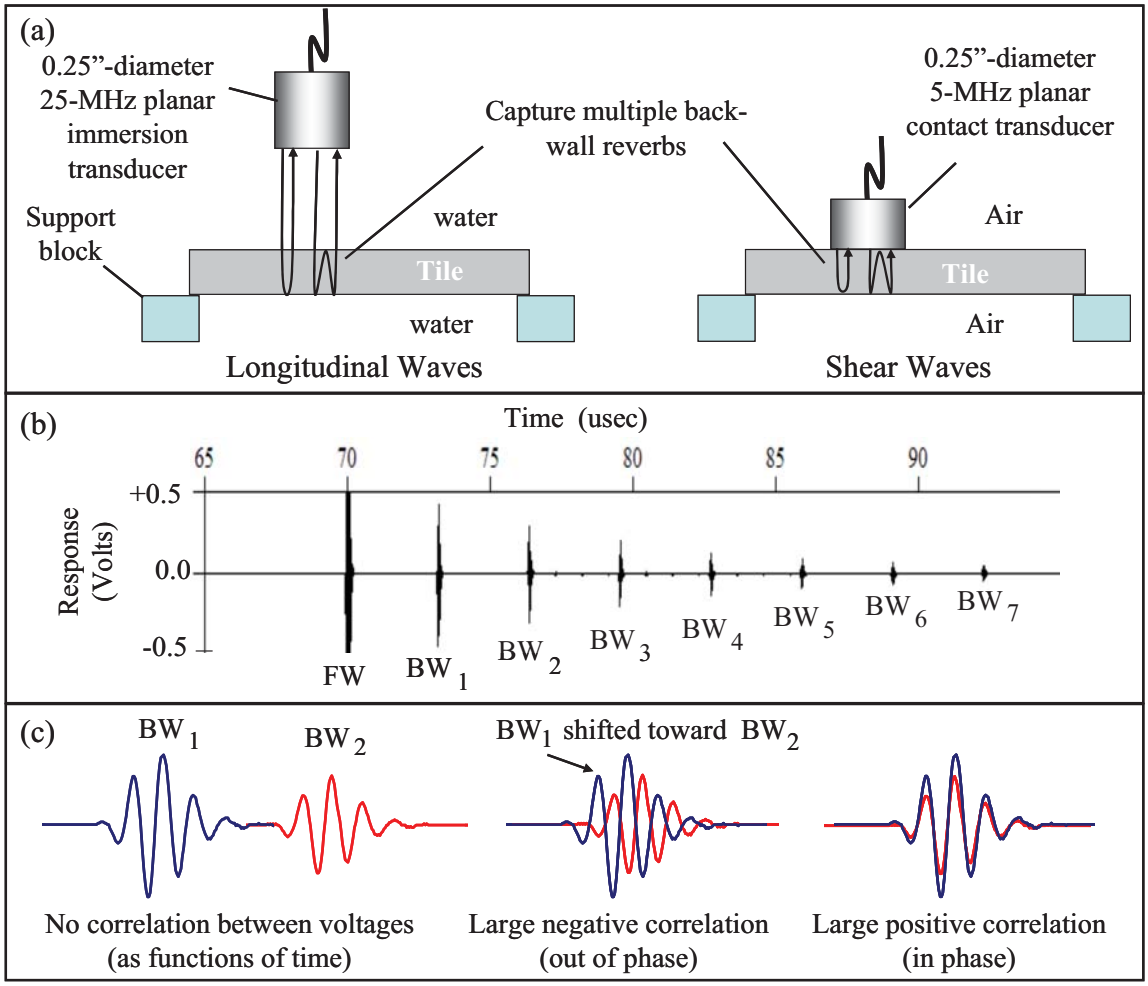

FIGURE 3. (a) Setups for ultrasonic velocity measurements. (b) Example of a measured waveform for the longitudinal case showing the front-wall echo and first seven back-wall reverberations. (c) Method of determining the time shift between two echoes by maximizing the correlation coefficient.

TABLE 1. Summary of ultrasonic velocity measurements. Tabulated shifts are relative to location A.

Tile	Measurement Location	Site Description	Longitudinal Velocity (cm/usec)	Shear Velocity (cm/usec)	Shift in Long. Velocity (percent)	Shift in Shear Velocity (percent)
415-3	A = Center	No Porosity	1.2169	0.7722	0.00	0.00
252-1	B = Edge	Little/No Porosity	1.2165	0.7721	-0.03	-0.02
252-1	C = Center	Moderate Porosity	1.1904	0.7560	-2.18	-2.11
281-4	D = Center	Moderate Porosity	1.2043	0.7647	-1.04	-0.98
281-4	E = Offset	High Porosity	1.1533	0.7334	-5.23	-5.03

(contact measurement using honey as a couplant).

Because of the low attenuation of the specimens many back-wall reverberation echoes could be observed at each measurement location, as illustrated in Figure 3b for one case. For each pair of such echoes, the difference in arrival times was determined using the correlation method illustrated in Figure 3c. The earlier of the two echoes in a pair was shifted to the right by an amount Δt, and the correlation coefficient between the two echoes was computed. The process was repeated to locate the time shift which maximized the correlation coefficient. An overall best estimate of the sound velocity was then computed using (twice tile thickness) / Δt_{ave}, where Δt_{ave} was an average of Δt values, typically obtained using the first 7 back-wall

echoes for longitudinal waves, and first 4 echoes for shear waves. The velocities measured in this manner are summarized in Table 1.

X-RAY MEASUREMENTS

Two types of X-ray examinations were made: (1) broad-area imaging to verify that regions of lower sound velocity were generally correlated with regions of lower density; and (2) detailed measurements of relative density at the same five sites where velocity was measured. The latter set of measurements enabled us to relate the sound velocity to the average porosity level in the through-thickness dimension.

The broad-area measurement setup is illustrated in Figure 4a. The diverging beam from a Phoenix xs|225 X-ray tube operating at 100 kVp passed through the ceramic tile and struck a digital X-ray imager. A lead mask (with a hole cut to accommodate the tile) reduced undercut from X-rays that would otherwise have passed by the edge of the tile and struck the imager. The local imager reading may be roughly equated to local X-ray intensity. Two X-ray images were made using the same equipment settings, one of the low-porosity reference tile (# 415-3) and one of a porous tile to be examined. These images were then digitally subtracted to emphasize density differences. The resulting image for porous tile 281-4 is shown in Figure 4b. The upper right corner of tile 281-4 has the highest received X-ray intensity, corresponding to the lowest average density. Note the similarity to the corresponding ultrasonic TOF image in Figure 2.

The second type of measurement, illustrated in Figure 5, was used to infer local values of tile density (and hence of tile porosity). There a tightly collimated X-ray beam (about 0.5 mm in diameter) at 180 kVp passed through a region of the tile and into a High-Purity Germanium (HPGe) X-ray detector. The transmitted intensity was measured as a function of X-ray energy. Three intensity measurements were made: (1) I_0 with no tile in place; (2) I_{ref} with the reference tile in place (i.e., at point A of the low-porosity tile 415-3); and (3) I_{test} with the test tile in place. At a given energy, we assume that the received X-ray intensity is proportional to $\exp(-\mu \cdot \rho \cdot h)$ where h is the thickness of the specimen, ρ is its density, and μ is an absorption coefficient dependent on the specimen chemistry (SiC in our case). From the set of three measurements one can deduce the ratio of the test specimen density to that of the reference specimen using:

$$\frac{\rho_{test}}{\rho_{ref}} = \frac{h_{ref}}{h_{test}} \bullet \frac{\ln\left[I_0(E)/I_{test}(E)\right]}{\ln\left[I_0(E)/I_{ref}(E)\right]} \quad . \tag{2}$$

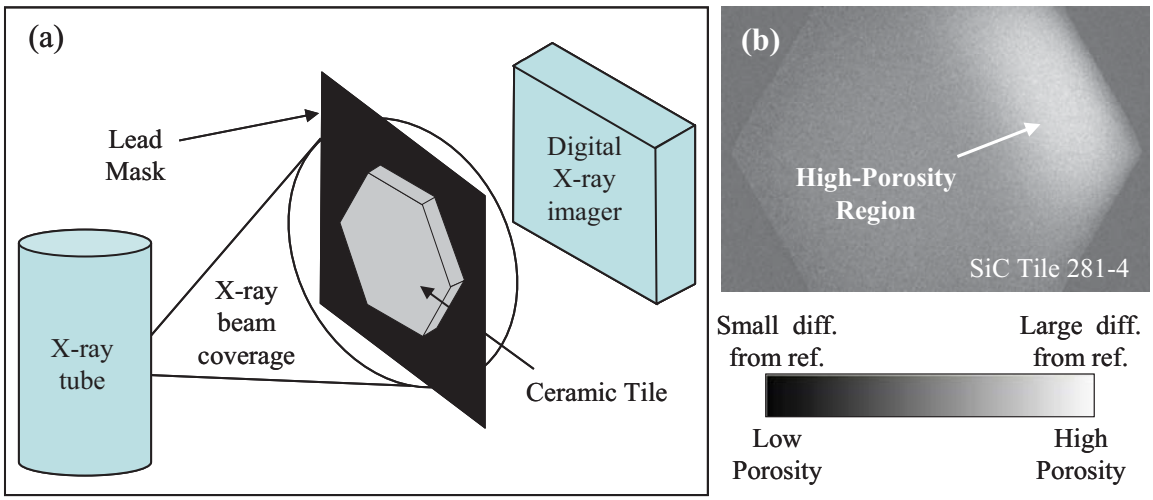

FIGURE 4. (a) Setup for X-ray large-area images. (b) X-ray image resulting from the digital subtraction of images from defective tile 281-4 and reference tile.415-3.

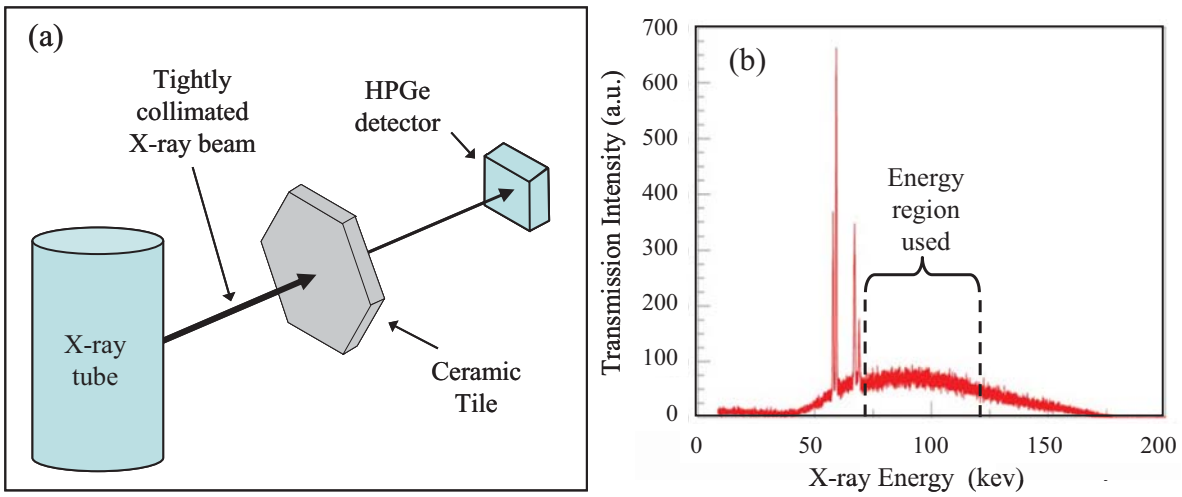

FIGURE 5. (a) Setups for X-ray relative density measurements. (b) Typical plot of measured X-ray intensity as a function of energy, showing the energy region used in the analysis.

TABLE 2. Results of X-ray relative density measurements. Velocity shifts from Table 1 have been repeated for convenience.

Tile	Measurement Location	Site Description	Relative Density	Percent Porosity	Shift in Long. Velocity (percent)	Shift in Shear Velocity (percent)
415-3	A = Center	No Porosity	1.0000	0.00	0.00	0.00
252-1	B = Edge	Little/No Porosity	0.9969	0.31	-0.03	-0.02
252-1	C = Center	Moderate Porosity	0.9762	2.38	-2.18	-2.11
281-4	D = Center	Moderate Porosity	0.9837	1.63	-1.04	-0.98
281-4	E = Offset	High Porosity	0.9548	4.52	-5.23	-5.03

This ratio was calculated for each energy point in the spectrum, and an average taken over the region indicated in Figure 5b to obtain our cited value. Results of our measurements are summarized in Table 2. There we have assumed that point A on the reference tile has "nominal" density (i.e., porosity = P = 0%), leading to relative porosity estimates at sites B, C, D and E. As usual, porosity (P) is defined here as the volume fraction occupied by the pores. Thus, within a localized volume under study, P = 0.1 or 10% means that the combined volume of all pores present equals 10% of the total volume. In Tables 1 and 2, estimated measurement uncertainties are about +/- 0.0004 cm/usec for velocity and +/- 0.0038 for relative density.

CORRELATION BETWEEN SOUND VELOCITY AND POROSITY

Many models exist which relate sonic velocity and porosity. For low porosity levels, the drop in velocity with increasing porosity can often be approximated using [3]:

$$V(P) \approx V(0)\,[1-aP]^{b} \quad . \tag{3}$$

Here V(P) is the velocity at porosity P, V(0) is the velocity without porosity, and the constants "a" and "b" depend on details of the models. For example in the Minimum Contact Area (MCA) Model as described by Mukhopadhyay and Phani [3], "a" and "b" are determined by the shape of the pores relative to the propagating sound beam as controlled by a shape parameter

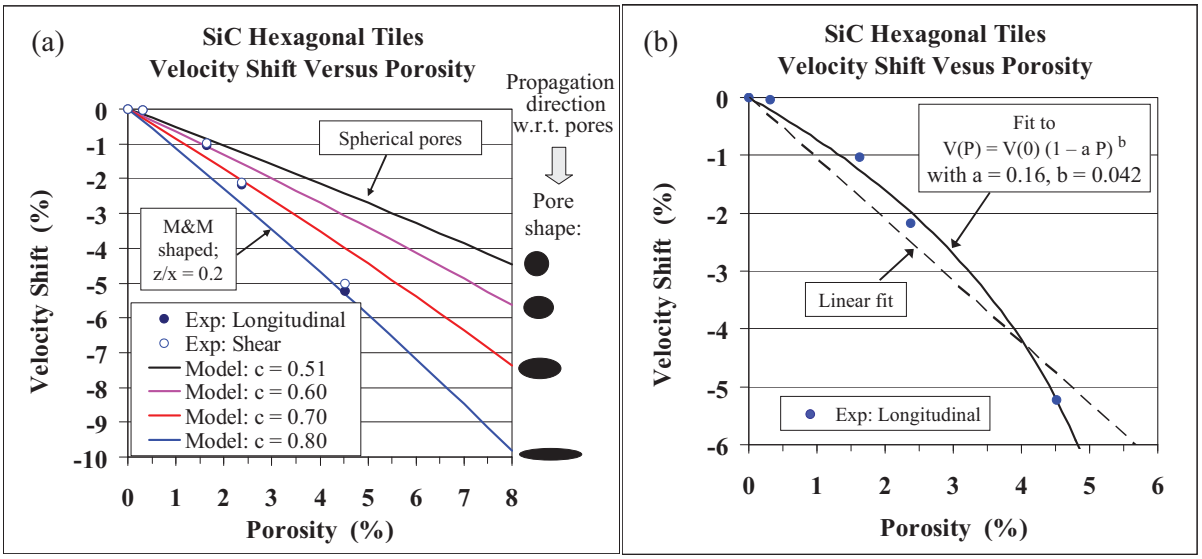

FIGURE 6. (a) Comparisons of measured velocity-versus-porosity data to the predictions of the Minimum Contact Area model. (b) Two fitted curves to the measured longitudinal wave data.

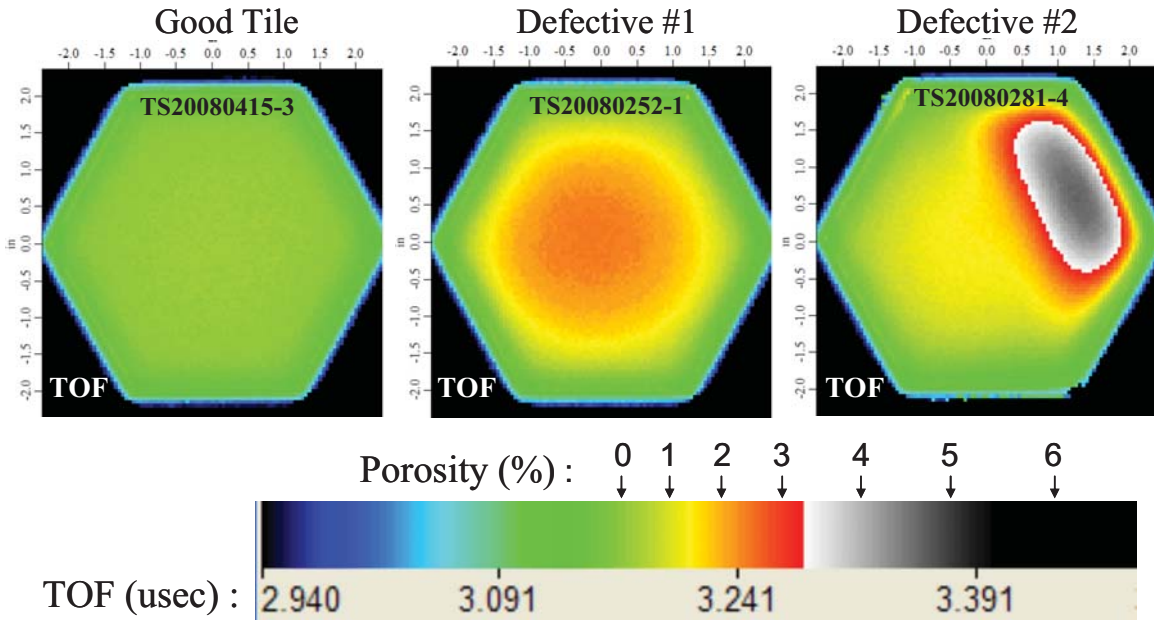

FIGURE 7. (a) Mapping of TOF values to porosity values for the three SiC ceramic tiles.

”c” . There “c” is determined by the aspect ratio of the pores, with c = 0.51 indicating spherical pores, and c > 0.51 indicating oblate spheroids. In Figure 6a we have compared our measured velocity-vs-porosity data to the predictions of the MCA model for four choices of the pore shape parameter. The four model curves are the same for longitudinal or shear waves. The measured rate of velocity drop, which is slightly smaller for shear waves than for longitudinal waves, is seen to lie between the predicted curves for “spherical pores” and “z/x = 0.2 oblate spheroids”. Note that pore shape is expected to influence the velocity-porosity curve. In addition pore shape may change during compaction, for example with pores beginning as eqiaxed shapes and progressing to elongated structures. Such shape changes during consolidation may be dependent on the details of the consolidation process used. Thus, the velocity-vs-porosity calibration curve is likely to be process dependent.

To translate the TOF C-scan images shown in Figure 2 into porosity images, two things are required. First, one must determine the setup-dependent time shift in Eq. (1). This allows

one to relate the local TOF values to local velocity values. Secondly, one must have a mapping function relating local longitudinal velocity to local porosity. t_{shift} can be determined by evaluating Eq. (1) using the measured velocity and TOF values at any one site. For our setup we found t_{shift} = 0.035 +/- 0.001 usec. The second condition can be satisfied by fitting a smooth function to the measured velocity-vs-porosity data. There it would be best to have many more (velocity, porosity) pairs than were acquired in our feasibility study. Nonetheless, for demonstration purposes, we can fit a smooth function through our sparse data, as shown in Figure 6b. Two fits are shown: (1) a linear fit which likely understates the velocity shift at high porosity levels; and (2) a fit to Eq. (3) which likely overstates the velocity shift at high porosity. Using the average of these two fits, we have translated the TOF C-scan images of Figure 2 into porosity images. The result is shown in Figure 7.

SUMMARY

Using traditional time-of-flight ultrasonic C-scans it is very easy to observe and document TOF variations produced by porosity in ceramic tiles. For the 0.75"-thick SiC tiles used in our demonstration a porosity level of a few tenths of a percent is readily observable. With relatively little additional work, conventional TOF images can be translated into percentage porosity images. The procedure is particularly easy for the ceramic tiles used in multi-layer armor because the tile thickness is carefully controlled. So long as "front-surface following" is used, we have found that the TOF images and hence the inferred porosity images are relatively insensitive to details of the ultrasonic inspection, such as the water path used, the degree to which the tile is level w.r.t. the scanning axes, and the focal length of the transducer. The resulting porosity images allow one to see at a glance which regions of the tile are well compacted and which are not. This could be useful for fine tuning a tile production process.

Finally we note that the porosity estimate at a given site is to be regarded as an average through the full thickness of the specimen, and the accuracy of the estimate is fairly insensitive to how the porosity is distributed. For example, for the mean velocity-vs-porosity calibration curve used here, the expected velocity shift is nearly the same for the case of 2 % porosity distributed uniformly through the thickness (1.9 % shift in velocity), and the case of 4 % uniform porosity confined to the top half of the specimen (2.1 % shift in average velocity).

ACKNOWLEDGEMENT

This Research was sponsored by the Army Research Laboratory and was accomplished under Cooperative Agreement Number W911NF-08-2-0036. The views and conclusions contained in this document are those of the authors and should not be interpreted as representing the official policies, either expressed or implied, of the Army Research Laboratory or the U.S. Government. The U.S. Government is authorized to reproduce and distribute reprints for Government purposes notwithstanding any copyright notation hereon.

REFERENCES

1. C. M. Sayers and R. L. Smith, "The Propagation of Ultrasound in Porous Media", *Ultrasonics* **20**, pp. 201-205 (1982).
2. F. J. Margetan, N. Richter, D. Barnard, D. Hsu, T. Gray, L. Brasche and R. Bruce Thompson, "Baseline UT Measurements for Armor Inspection", Rev. of Prog. in QNDE, Vol. 29, eds. D.O. Thompson and D.E. Chimenti, (AIP, Melville NY, 2010), pp. 1217-1224.
3. A. K. Mukhopadhyay and K. K. Phani, "An Analysis of Microstructural Parameters in the Minimum Contact Area Model for Ultrasonic Velocity-Porosity Relations", *J. of the Euro. Ceramic Soc* **20**, pp. 29-39 (2000).